

A Self-calibration Method for the Edge Thomson Scattering Diagnostic in ITER

Eiichi Yatsuka, Takaki Hatae, Yoshinori Kusama

Japan Atomic Energy Agency

(Received: 20 November 2009 / Accepted: 5 January 2010)

Calibration of spectral transmissivity of the collection and transmission optics is one of the most crucial issues for the Thomson scattering diagnostic system. Radioactivation of the vacuum vessel in ITER makes it difficult to calibrate spectral transmissivity in areas near the vacuum vessel. By using an additional calibration laser whose wavelength differs from those of the diagnostic laser and equipping two lasers with Thomson scattering lights, we can obtain the electron temperature and the relative transmissivity of each spectral channel of the polychromator from the Thomson scattering signal itself. A ruby laser is a promising candidate as a calibration laser because the wavelength does not diverge greatly from that of a diagnostic laser and from the lower limit of an observable wavelength. Even if the signal-noise ratio degrades, the available electron temperature data during calibration operations remain largely unaffected. A degrading signal-noise ratio increases statistical error in electron temperature data and relative spectral transmissivity. Even when the spectral transmissivity is unknown, electron temperature data may be obtained within a 10% margin of error, which fulfills the requirements for edge electron temperature measurement in ITER.

Keywords: Thomson scattering, ITER, Self-calibration, Spectral transmissivity, Statistical error analysis

1. Introduction

Incoherent Thomson scattering diagnostics is a standard method to measure profiles of electron temperature T_e and electron density n_e in fusion plasmas. The edge Thomson scattering diagnostics for ITER is required to measure the region in which $r/a > 0.85$, where r and a denote the minor radii of a measurement point and the separatrix, respectively. Errors in edge plasma diagnostics are required to be less than 10% for T_e and 5% for n_e in the range of 50 eV to 10 keV, and 5×10^{18} to $3 \times 10^{20} \text{ m}^{-3}$, respectively [1]. To satisfy these requirements, it is necessary to develop a high-power laser and high-performance spectroscopic optics. A 5-J, 100-Hz YAG laser will be installed for the edge Thomson scattering system [2], so a polychromator system will be employed to analyze the spectrum for Thomson scattering.

Optimization of the band pass filters of the polychromator for the edge Thomson scattering system in ITER was examined by Kajita [3,4]. In this optimization, the errors of T_e and n_e were evaluated relative to the error in the number of detectable photons for each spectral channel. However, the deterioration in spectral transmissivity by browning as a result of neutron and gamma ray irradiation and chemical sputtering, was not considered. Deterioration in spectral transmissivity causes not only a drop in the total number of detectable photons but also introduces severe systematic error in the

measurement of T_e . For instance, if the deterioration of transmissivity in the shorter-wavelength region is larger than that in the longer-wavelength region, T_e will be observed as a lower value than the true T_e . An *in-situ* self-calibration method of relative transmissivity of the optical systems for Thomson scattering diagnostics was proposed by Smith [5]. In this method, a calibration laser having a different wavelength from that of the diagnostic laser is applied to evaluate the relative transmissivity of each spectral channel of the polychromator, which can be calibrated by the Thomson scattering signal.

We applied Smith's method for the edge Thomson scattering system in ITER. The objectives of this work are to clarify what kind of laser is promising, to evaluate how hot and dense the plasma needs to be for the self-calibration operation and to evaluate the magnitude of the statistical error of parameters related to the self-calibration method. We evaluated the statistical error of T_e and $n_e C_j$ numerically, where j designates a spectral channel and C_j denotes the transmissivity deterioration factor (< 1) from baseline, i.e. at calibration. Section 2 describes how to simulate experiments and to apply the self-calibration method to the edge Thomson scattering system in ITER. In section 3, the statistical error of the self-calibration method is evaluated and its availability is verified through similar procedures via experimental data analysis. Conclusions are described in section 4.

author's e-mail: yatsuka.eiichi@jaea.go.jp

2. Calculation of the edge Thomson scattering diagnostics

Figure 1 shows the flow chart of the numerical experiments. At first, we assumed T_e , n_e and C_j . A set of band-pass filters of the polychromator was previously determined to minimize the maximum error of T_e in $50 \text{ eV} < T_e < 10 \text{ keV}$ when $n_e = 5 \times 10^{18} \text{ m}^{-3}$, a condition which yields the highest degree of statistical error because of the minimum detectable number of photons. Signal and noise were evaluated using the configuration and parameters of edge Thomson scattering in ITER, as shown in Fig. 2 and Table 1, respectively. Statistical error in the number of detectable photons is used to calculate the signal variable and was computed by using a random number whose shape is Gaussian with a standard deviation of $\sigma_{j,L}$, as defined in Eqs. (1), (2) and (4). Thereafter, T_e and $n_e C_j$ were fitted through the least-squares method, and these parameters subsequently were compared with assumed values.

The number of photons due to Thomson scattering from the laser L detected in the j th spectral channel $N_{S,j,L}$ ($L = M$ (main), C (calibration)) can be written as

$$\begin{aligned} N_{S,j,L} &= C_j n_e r_e^2 \Delta l \frac{\lambda_{i,L} E_{i,L}}{hc} \Omega \int_{\varepsilon_{j1,L}}^{\varepsilon_{j2,L}} S(\varepsilon_L, \theta, 2\alpha) \eta(\varepsilon_L) T(\varepsilon_L) d\varepsilon_L \\ &\equiv C_j n_e g_{j,L}(T_e), \end{aligned} \quad (1)$$

where h , c , $S(\varepsilon_L, \theta, 2\alpha)$, $\eta(\varepsilon_L)$ and $T(\varepsilon_L)$ denote the Planck constant, light speed, the spectral density of

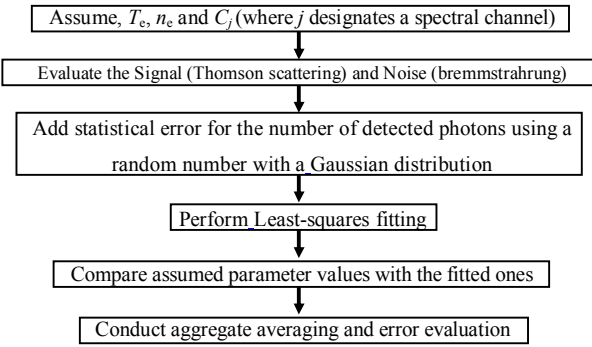


Fig. 1 Flow chart of numerical calculations.

Table 1 Parameter list

symbol	meaning	value
$E_{i,M}$	Main laser pulse energy	5 J
$\lambda_{i,M}$	Wavelength of main laser	1064 nm
d_i	Laser diameter	5 mm
Δl	Scattering length	5 mm
Ω	Solid angle	10 msr
θ	Scattering angle	140°
Z_{eff}	Effective charge number	3
K_e	Enhancement factor	2
Δt	Gate opening time	30 ns
D	Effective length of plasma	4.5 m

Thomson scattering [6,7], the quantum efficiency of the avalanche photo diode (APD) and spectral transmissivity of optics, respectively; and $\varepsilon_L \equiv (\lambda_s - \lambda_{i,L})/\lambda_{i,L}$ (λ_s and $\lambda_{i,L}$ denotes the scattered and incident wavelengths of laser L, $2\alpha \equiv m_e c^2 / \kappa T_e$ (m_e and κ denote the electron rest mass and the Boltzmann constant), respectively). The normalized wavelengths $\varepsilon_{j1,L}$ and $\varepsilon_{j2,L}$ correspond to the lower and upper wavelength boundaries of the j th spectral channel. Other nomenclature is shown in Table 1. Wavelength dependence upon spectral density in the case of $T_e = 10 \text{ keV}$, which corresponds to the upper requirement

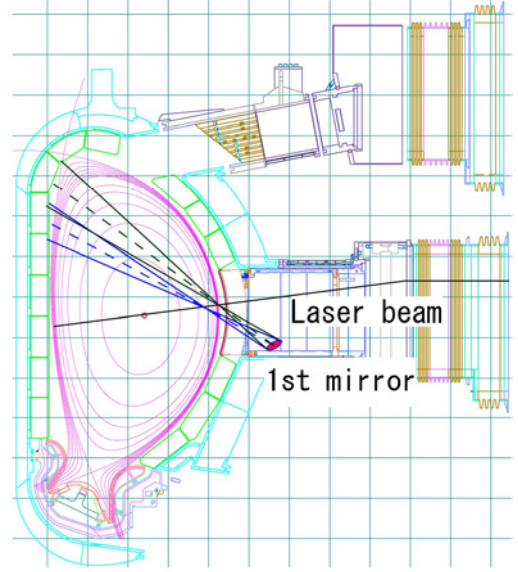


Fig. 2 Configuration of edge Thomson scattering diagnostic system.

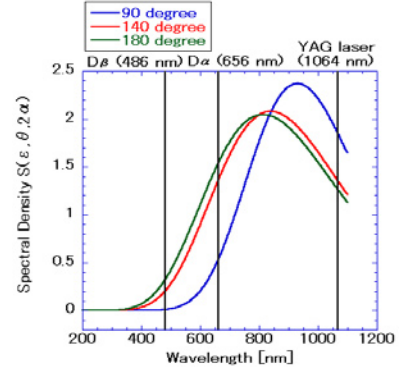


Fig. 3 Spectrums of Thomson scattering when $T_e = 10 \text{ keV}$.

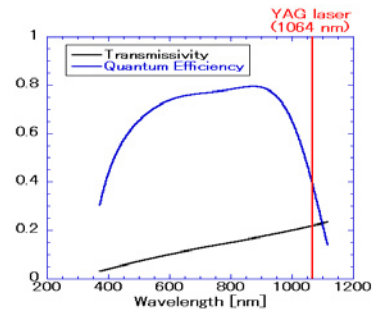


Fig. 4 Assumed transmissivity and quantum efficiency of APD.

of edge T_e measurements in ITER, is shown in Fig. 3. In the case of 140 degree scattering, which approximately corresponds to the edge Thomson scattering diagnostics in ITER, the lower range of the spectrum of Thomson scattering lies around D_β line (486 nm). Figure 4 shows the simulated quantum efficiency of the APD (Hamamatsu Photonics SPL 5068) and transmissivity of optics (1 Rhodium mirror, 2 Aluminum mirrors and Fluorine-doped silica core OH-free optical fiber [8]).

For background noise, we considered only bremsstrahlung radiation. An intense line spectrum, e.g. D_α (656 nm), increases the level of background radiation. Therefore, we fixed the boundary of a band-pass filter (a segment of the polychromator) at 656 nm to reduce the D_α line spectrum. In addition, to reduce the D_β line spectrum we limited the lower limit of the observed wavelength so that it is not shorter than 486 nm. In this way, we eliminated the two most dominant line spectra using the band-pass filter. The spectrum of bremsstrahlung is written as

$$N_{B,j} = C_j d_i A L \sin \theta \Omega_s \Delta t K_e \int_{\varepsilon_{j,M}}^{\varepsilon_{j,M}} j(\varepsilon_M) \eta(\varepsilon_M) T(\varepsilon_M) \frac{\lambda_{i,M}(1 + \varepsilon_M)}{hc} d\varepsilon_M, \quad (2)$$

where

$$j(\varepsilon_M) = \frac{8}{3} r_e^3 \frac{m_e c^2}{\lambda_{i,M}(1 + \varepsilon_M)^2} n_e^2 Z_{\text{eff}}^2 \sqrt{\frac{2m_e c^2}{\pi \kappa T_e}} \exp\left(-\frac{hc}{T_e \lambda_{i,M}(1 + \varepsilon_M)}\right) \times \ln\left(\frac{4T_e \lambda_{i,L}(1 + \varepsilon_L) \gamma}{hc}\right), \quad (3)$$

where γ denotes the Euler's constant, and K_e denotes the enhancement factor representing the difference between the theoretical and measured bremsstrahlung intensities arising due to the multi-reflection in the vacuum vessel and impurity radiation. The Gaunt factor was evaluated using a low-frequency Born approximation [9]. In equations (2) and (3), the wavelength is normalized so that it corresponds to that of the main laser as a matter of convenience. In this paper, the special integration of the bremsstrahlung was approximated using the averaged value on the viewing path, i.e. $T_e = 12$ keV, $n_e = 1.2 \times 10^{20} \text{ m}^{-3}$ and the effective length of the plasma $D = 4.5$ m, respectively [3, 10].

Since $N_{S,j,L}$ is proportional to both n_e and C_j , we cannot obtain n_e and C_j independently solely from the Thomson scattering lights. Obtainable parameters through the application of Smith's self-calibration method are T_e and $n_e C_j$. The number of unknown parameters is 1 plus the number of spectral channels. If the main and calibration lasers are fired at different times, the number of obtainable signals ($2 \times$ the number of spectral channels) is sufficient to fit all unknown parameters. Thus, we need to measure the Thomson scattering lights from the main and calibration lasers separately. A conceptual timing chart of the self-calibration method is shown in Fig. 5.

A typical value of statistical error for the number of detectable photons due to Thomson scattering is represented as

$$\sigma_{j,L}^2 = N_{S,j,L} + 2N_{B,j}, \quad (4)$$

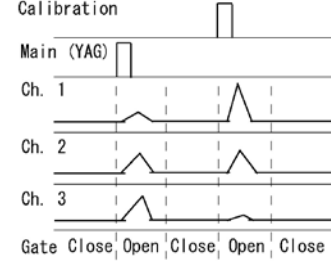


Fig. 5 Conceptual timing chart of the self-calibration method. For simplicity, a 3-spectral channel system is assumed. The waveform will be distorted due to the characteristics of the APD circuit, e.g. capacitance. In this example, the fitted parameters are T_e , $n_e C_1$, $n_e C_2$ and $n_e C_3$, (1+3 parameters) whereas the obtainable parameters are $N_{S,1,M}$, $N_{S,2,M}$, $N_{S,3,M}$, $N_{S,1,C}$, $N_{S,2,C}$, and $N_{S,3,C}$ (2×3 parameters).

where the second factor of the arriving photons due to bremsstrahlung indicates that the Thomson scattering signal, detected experimentally, will contain background radiation. Therefore, we need to subtract this signal from the values of a signal without Thomson scattering light, i.e. background light. We investigated the effect of bremsstrahlung on the validity and availability of the self-calibration method.

In this paper, the polychromator was designed to be optimized for standard experiments; i.e., only the main laser is considered and the transmissivity deterioration factor C_j is assumed to have a value of 1 for all spectral channels. With the Gaussian assumption, the probability $P(T_e, n_e)$ of observing X_j with a standard deviation $\sigma_{j,L}$ for observations about the true value $N_{S,j,L}(T_e, n_e)$ is

$$P(T_e, n_e) = \prod_j \left(\frac{1}{\sigma_{j,M} \sqrt{2\pi}} \right) \exp\left\{ -\frac{1}{2} \left[\frac{X_j - N_{S,j,L}(T_e, n_e)}{\sigma_{j,M}} \right]^2 \right\}, \quad (5)$$

so that one can obtain the most probable T_e and n_e by minimizing the following χ^2 [11, 12]:

$$\chi^2 = \sum_j \left[\frac{X_j - N_{S,j,L}(T_e, n_e)}{\sigma_{j,M}} \right]^2. \quad (6)$$

Since the first term of Eq. (5) is the normalized parameter, the statistical error for T_e and n_e is evaluated from χ^2 . The parameter χ^2 may be paraboloid around the most probable T_e and n_e . Thus, we defined the statistical error of T_e and n_e through a Taylor expansion of χ^2 around the minimum value χ_0^2 and assigned 1 for deviations from χ_0^2 :

$$\sigma_{T_e}^2 = 2 \left| \frac{\partial \chi^2}{\partial T_e^2} \right|^{-1} = \left[\sum_j \frac{n_e^2}{\sigma_{j,M}^2} (g'_{j,M}{}^2 - g_{j,M} g''_{j,M}) \right]^{-1}, \quad (7)$$

$$\sigma_{n_e}^2 = 2 \left| \frac{\partial \chi^2}{\partial n_e^2} \right|^{-1} = \left[\sum_j \frac{g_{j,M}^2}{\sigma_{j,M}^2} \right]^{-1}, \quad (8)$$

where $g'_{j,M}$ and $g''_{j,M}$ denote the first and second

derivatives of $g_{j,M}$ with respect to T_e , respectively. The polychromator was optimized in order to minimize the maximum statistical error of T_e in $50 \text{ eV} < T_e < 10 \text{ keV}$ when $n_e = 5 \times 10^{18} \text{ m}^{-3}$. Figure 6 shows the dependence of T_e upon the statistical error of the optimized polychromator. A band-pass filter of optimized segments is summarized in Table 2. We used this polychromator for evaluating the self-calibration method.

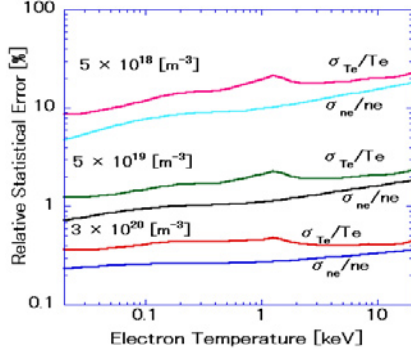


Fig. 6 Relative statistical errors of optimized polychromator.

Table 2 Optimized polychromator segments.

Channel No.	Center [nm]	Width [nm]
1	571	170
2	759	206
3	897.8	71.6
4	995.1	123
5	1060.3	7.4
6	1070	12

3. Availability of the self-calibration method

In this section, we investigated the availability of the self-calibration method in a manner similar to the earlier data analysis experiments. The self-calibration method does not need to be available over the entire range of values for the parameters T_e and n_e . Moreover, in principle, we should not require knowing the values of T_e and n_e for a plasma during self-calibration operations.

The overlap of spectra of the main and calibration lasers enables us to calibrate the spectral transmissivity in the self-calibration method. We investigated three lasers as candidates for a calibration laser: a second harmonic YAG laser (2 J, 532 nm), a ruby laser (5 J, 694.3 nm) and an alexandrite laser (1.5 J, 800 nm). Their pulse energies were assumed from past performance of commercial lasers of each type. Since the optimized polychromator (see Table 2) does not have a segment around the wavelength of the second harmonic of the YAG laser, we investigated the effect of an additional segment inserted at 532 nm. As shown in Fig. 7, T_e at calibration was well fitted using an Alexandrite laser ($> 0.5 \text{ keV}$) and a Ruby ($> 1.5 \text{ keV}$) laser as calibration lasers. On the other hand, if the second harmonic YAG laser were used as a calibration laser, we

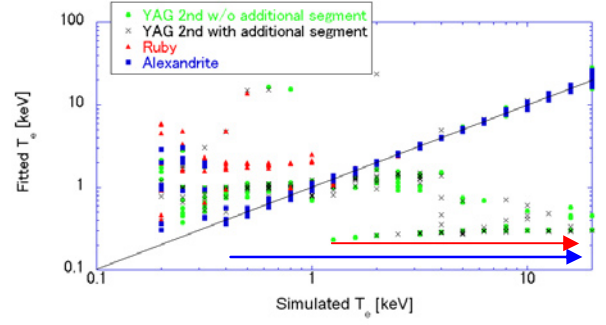


Fig. 7 Relationship between calibration laser and statistical error of T_e . An additional segment was set at 532 nm, which coincides with the wavelength of the second harmonic YAG laser. The blue (red) arrow shows the available T_e with an alexandrite (ruby) laser.

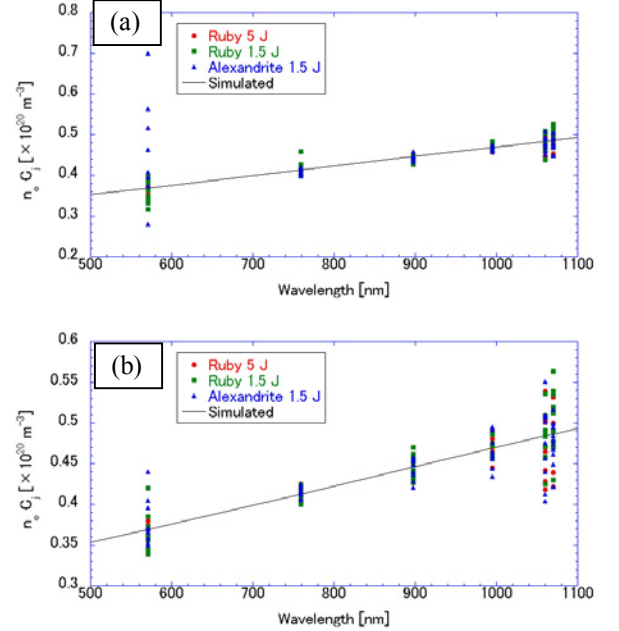


Fig. 8 Re-construction of relative transmissivity when (a) $T_e = 2 \text{ keV}$ (b) $T_e = 10 \text{ keV}$.

could obtain a simulated value for T_e even when T_e exceeds 10 keV, which corresponds to the upper requirement of edge T_e measurements. Since the additional segment did not essentially improve the results of the fitting, it is suggested that this is not caused by the problem of optimization of the polychromator. If the second harmonic YAG laser were used as a calibration laser, then whether we can calibrate T_e or not depends on the unavoidable error of the detected, arriving photons in the edge Thomson scattering diagnostics in ITER. In this simulation, n_e was assumed to be $5 \times 10^{19} \text{ m}^{-3}$. On the other hand, Pacher predicted n_e and T_e to be approximately equal to $5.5 \times 10^{19} \text{ m}^{-3}$ and 3.5 keV, respectively, at the separatrix of an H-mode plasma [10]. If a calibration is carried out using an H-mode plasma, an alexandrite laser

and a ruby laser will be useful for calibrating T_e . Since the wavelength of the second harmonic YAG laser is so far from the main (fundamental YAG) laser's wavelength, the spectra of the main and calibration lasers hardly overlap. Therefore, we concluded that the second harmonic YAG laser is not promising as a calibration laser in edge Thomson scattering in ITER.

Note that for evaluating the availability of the self-calibration method, it is important to re-construct not only T_e but also all $n_e C_j$. Figure 8 shows the relationship between the fitted and simulated relative spectral transmissivity. We compared a ruby and an alexandrite laser because they are promising candidates as calibration lasers from the view point of T_e fitting. A ruby laser gives significantly less error for the shortest spectral channel of the polychromator compared to an alexandrite laser when T_e at calibration is relatively low (less than several keV). This tendency remained true even when the power of the ruby and an alexandrite lasers was the same. Thus, we concluded that the wavelength is the most important parameter for determining the calibration laser. In addition, a ruby laser is one of the most promising lasers because its wavelength does not differ much from that of the main laser and from the lower limit of measured wavelengths. In addition, the fixed segment (656 nm) to reject the intense line spectrum of D_α is near the wavelength of the ruby laser (694.3 nm). As such, one may not have to add an extra segment to the polychromator for the self-calibration method.

We investigated the statistical error of the parameters obtained through the self-calibration method. We carried out numerous trials (100 times) to evaluate the validity and availability of the self-calibration method while changing the initial condition of the random number creation. Results indicate that T_e may be obtained within an adequate margin of statistical error ($< 10\%$) from a single calibration operation using a 5-J ruby laser. If the absolute transmissivity of a spectral channel is obtained, then it is possible to obtain values for all other spectral channels. Table 3 shows the results when T_e equals 2 keV. Results do not change significantly when T_e equals 10 keV, the upper limit requirement for edge T_e measurements. Therefore, if it is necessary to obtain relative spectral transmissivity with a smaller margin of error than that of the normal deviation, we should collect data from all calibration operations and average the results.

Since the transmission regions of band-pass filters for long-wavelength spectral channels of the polychromator are much narrower than those of short-wavelength channels, the statistical error of relative spectral transmissivity in the long-wavelength region may be reduced by incorporating these channels. Figure 9 shows the effect of incorporating the long-wavelength channels with a simulated T_e of 2 keV. The statistical error of relative spectral transmissivity can be reduced by

Table 3 Statistical errors of fitted parameters. The number of trials is 100.

Value	Simulated	Fitted Mean	Normal Deviation
T_e [keV]	2.00	2.01	65 eV (3.80 %)
$n_e C_1$ (486-656 nm) [10^{20}m^{-3}]	0.369	0.369	0.0087 (2.37 %)
$n_e C_2$ (656-862 nm) [10^{20}m^{-3}]	0.413	0.413	0.0059 (1.42 %)
$n_e C_3$ (862-933.6 nm) [10^{20}m^{-3}]	0.446	0.446	0.0101 (2.26 %)
$n_e C_4$ (933.6-1056.6 nm) [10^{20}m^{-3}]	0.469	0.469	0.0058 (1.24 %)
$n_e C_5$ (1056.6-1064 nm) [10^{20}m^{-3}]	0.484	0.482	0.0227 (4.68 %)
$n_e C_6$ (1064-1076 nm) [10^{20}m^{-3}]	0.486	0.488	0.0185 (3.80 %)

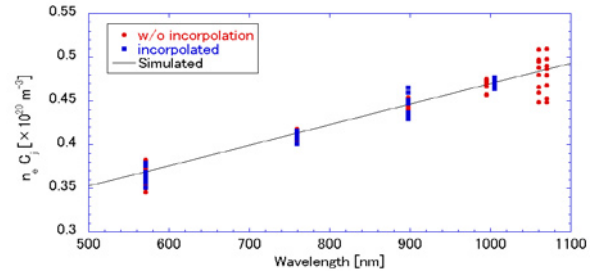


Fig. 9 By incorporating 3 longest-wavelength channels of the polychromator, the statistical error of relative spectral transmissivity was reduced.

incorporating the narrow spectral channels. However, these narrow spectral channels play a crucial role in determining a relatively low T_e . As such, it remains unclear whether obtaining averaged relative spectral transmissivity using multi-channel data is the best method.

Since the signal-noise ratio decreases by a decrement of n_e , we investigated the availability of the self-calibration method for low n_e operations. As shown in Fig. 10 (a), the lower limit of T_e during calibration operations does not change even when n_e decreases by 80%. On the other hand, the statistical error at high (> 5 keV) T_e became worse because of a decrease in the detectable number of photons at longer-wavelength spectral channels of the polychromator; i.e., the detectable number of photons due to bremsstrahlung is relatively low because of the narrow transmission region. The detectable number of photons due to Thomson scattering of the main (YAG) laser becomes large when T_e is low. Therefore, even if n_e becomes small, the lower limit of available T_e for self-calibration does not change. As expected, the ratio of the relative error for relative spectral transmissivity became small as n_e increased (see Fig. 10 (b)).

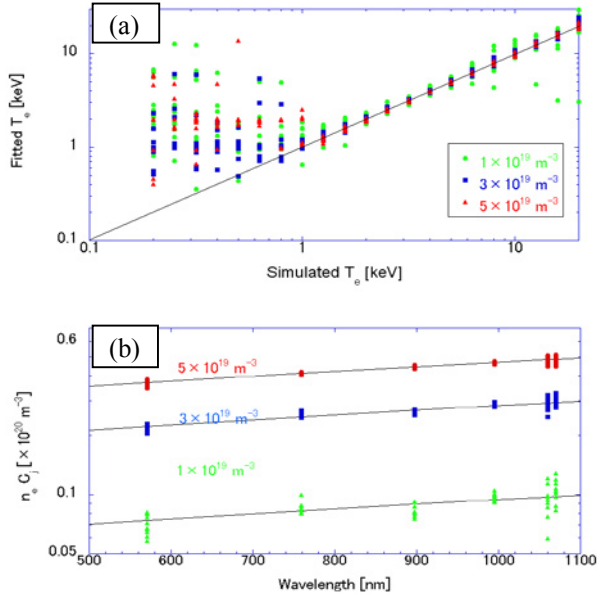


Fig. 10 Relationship between statistical error of (a) T_e (b) relative spectral transmissivity and n_e .

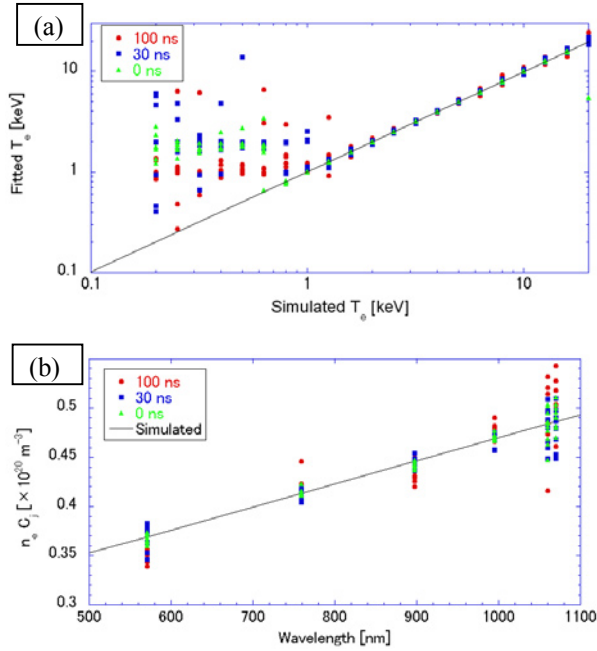


Fig. 11 Relationship between statistical error of (a) T_e (b) relative spectral transmissivity and gate opening time of collection optics.

Since the detectable number of photons due to bremsstrahlung will be much greater (10 times or more) than that due to Thomson scattering in ITER edge Thomson scattering diagnostics, the effect of bremsstrahlung on statistical error should be evaluated. As shown in Fig. 11 (a), if we neglect the effect of bremsstrahlung, the available T_e for calibration dropped to less than 1 keV. On the other hand, there is a slight increase in the lower limit of T_e for calibration when the gate opening time becomes 100 ns, which corresponds to

the collection optics of the Thomson scattering system in the JT-60U. The statistical error of relative spectral transmissivity rises as the gate opening time increases (see Fig. 11 (b)). However, results indicate that the error did not significantly worsen. The gate opening time will not limit the available conditions for calibration operations of the edge Thomson scattering diagnostics in ITER.

4. Conclusions

Calibration of spectral transmissivity of collection and transmission optics is one of the most crucial issues for the Thomson scattering diagnostic system. By using an additional laser with a different wavelength from that of the main diagnostic laser and fitting two Thomson scattering signals from both lasers separately, we can calibrate relative spectral transmissivity. Since an overlap in the spectra of the main and calibration lasers enables the reflection of both electron temperature and spectral transmissivity in the shape of a spectrum, the availability of this method depends on the wavelength of the additional laser. A Ruby laser is promising because its wavelength does not differ significantly from that of both the main (YAG) laser and from the lower observable limit. The electron temperature and electron density suitable for calibration exceed 1.5 keV and several 10^{19} m^{-3} , respectively. Even when the spectral transmissivity is unknown, we can obtain an electron temperature within a 10% margin of error, which corresponds to the requirements of edge temperature measurements in ITER.

Acknowledgements

One of the authors (E. Y.) thank the members of ITER Diagnostic Group in Japan Atomic Energy Agency for useful discussion and informative comments.

- [1] A. J. Donne *et al.*, Nucl. Fusion **47**, S337 (2007); recently, required observation region was changed to $r/a > 0.85$.
- [2] T. Hatae *et al.*, Trans. Fusion Sci. Technol. **51**, 58 (2007).
- [3] S. Kajita *et al.*, Rev. Sci. Instrum. **79**, 10E726 (2008).
- [4] S. Kajita *et al.*, Fusion Eng. Des. **84**, 2214 (2009).
- [5] O. R. P. Smith *et al.*, Rev. Sci. Instrum. **68**, 725 (1997).
- [6] T. Matoba *et al.*, Japan. J. Appl. Phys. **18**, 1127 (1979).
- [7] O. Naito *et al.*, Phys. Fluids **B 5**, 4256 (1993).
- [8] T. Kakuta *et al.*, J. Nucl. Mater. **307-311**, 1277 (2002).
- [9] I. H. Hutchinson, *Principles of Plasma Diagnostics* (Cambridge University Press, Cambridge, 2002) p. 197.
- [10] G. W. Pacher *et al.*, Plasma Phys. Controlled Fusion **46**, A257 (2004).
- [11] P. R. Bevington, D. K. Robinson *Data Reduction and Error Analysis for the Physical Sciences* (Mc-Graw-Hill, New York, 2003) p. 104.
- [12] A. P. Millar *et al.*, Plasma Phys. Controlled Fusion **42**, 337 (2000).